GEOMICROBIOLOGY JOURNAL
https://doi.org/10.1080/01490451.2019.1641770

Taylor & Francis
Taylor & Francis Group

'Follow the Water': Hydrogeochemical Constraints on Microbial Investigations 2.4 km Below Surface at the Kidd Creek Deep Fluid and Deep Life Observatory

Garnet S. Lollar[a], Oliver Warr[a], Jon Telling[a], Magdalena R. Osburn[b], and Barbara Sherwood Lollar[a]

[a]Department of Earth Sciences, University of Toronto, Toronto, Ontario, Canada; [b]Department of Earth and Planetary Sciences, Northwestern University, Evanston, IL, USA

ABSTRACT

Microbiological and geochemical data are presented to characterize the hydrogeochemistry and to investigate extant microbial life in fracture waters 2.4 km below surface, at the Kidd Creek Observatory in Canada. Previous studies identified the world's oldest groundwaters with mean residence times on the order of millions to billions of years trapped in fractures in Precambrian host rock here. In this study, major ion chemistry, $\delta^{18}O$ and $\delta^{2}H$ isotopic signatures and dissolved gases in the fracture waters are shown to be distinct from potential contamination end-members, demonstrating the fracture waters are not impacted by waters used in mining operations. A previous work on sulfur isotope signatures suggested a longstanding indigenous population of sulfate-reducing bacteria in these highly reducing fluids and sufficient sulfate to support microbial activity. Here, we report the first evidence for extant visible and cultivable microbial life at this location. Anaerobic metabolisms were investigated using the Most Probable Number (MPN) method. The fracture fluids contained extant cells at low biomass density ($\sim 10^{3}$–10^{4} cells/mL) and showed a strong response from autotrophic sulfate-reducers and alkane-oxidizing sulfate reducers. These lines of evidence provide the interpretational framework (chemical, hydrogeologic, and microbiologic) essential to the on-going genomic and metagenomic investigations at the Kidd Creek Observatory – the world's most longstanding location for investigation of subsurface fluids and deep life at such profound depth.

ARTICLE HISTORY
Received 15 January 2019
Accepted 1 July 2019

KEYWORDS
Deep life observatory; groundwater; habitability; most probable number; subsurface biosphere

Introduction

Humankind's existence as organisms exclusively inhabiting the surface of the Earth has long biased our assumptions about the distribution of subsurface life (NASEM 2018). Even in the modern scientific era, the planet's biosphere was thought of as a thin veneer on or near the surface of the planet (Jannasch and Taylor 1984), with life primarily dependent on photosynthesis to thrive. An exciting scientific revolution began with the discovery, in the late 1970s, of chemoautotrophic microbial communities associated with hydrothermal vents on the ocean floor. Since that time rock-hosted chemoautotrophic life has been found to not only be a "deep hot biosphere" but sustainable via the products of lower temperature water–rock reactions (<100°C), and, hence, a phenomenon found not only at high temperature vents but at off-axis spreading centers (Bach and Edwards 2003; Kelley et al. 2005; Proskurowski et al. 2008) and cool continental settings, including the Precambrian cratons (see reviews by Onstott 2016; Schrenk et al. 2013; and references therein).

Major questions about the nature and distribution of the subsurface biosphere nonetheless remain, including delineating the variety and sources of electron donors and electron acceptors sustaining deep subsurface microbiomes, and the variety and relative importance of microbial metabolisms (Bomberg et al. 2015; D'Hondt et al. 2009; Osburn et al. 2014; Pedersen et al. 2014; Purkamo et al. 2015; Simkus et al. 2016; Telling et al. 2018). Recent progress has been made in models extrapolating what is known about cell density, porosity and permeability, attached versus unattached biomass ratios, and power scaling laws to revise estimates of subsurface biomass (Kallmeyer et al. 2012; Lipp et al. 2008; Magnabosco et al. 2018a; McMahon and Parnell 2014) but the paucity of measurements remains a common theme in all these studies. This knowledge gap is particularly large for the terrestrial subsurface, and particularly so for crystalline rock settings at great depth (2–3 km), where fracture waters are isolated from the surface photosphere on geologic timescales. These "dark energy" systems where chemolithotrophy plays an important role in sustaining habitability are vital to our understanding of life's ability to sustain ecosystems where cell abundance and biomass are both exceedingly low (Edwards et al. 2012; Schrenk et al. 2013). Cell division has been estimated to take place at rates 10^{4}–10^{6} fold more slowly in these geologically ancient, oligotrophic environments compared to surface ecosystems

CONTACT Barbara Sherwood Lollar barbara.sherwoodlollar@utoronto.ca Department of Earth Sciences, University of Toronto, 22 Russell Street, Toronto, Ontario M5S 3B1, Canada
*Current address: School of Natural and Environmental Sciences, Newcastle University, Drummond Building, Newcastle NE1 7RU, UK

(Hoehler and Jorgensen 2013; Labonté et al. 2015). These realms of the "hidden hydrogeosphere" (Warr et al. 2018) remain a major frontier in the exploration for life on Earth (Magnabosco et al. 2018b; McMahon and Parnell 2014) and provide important analog environments for planetary scientists and astrobiologists considering the potential for subsurface life on Mars and elsewhere in the solar system (Michalski et al. 2017; NASEM 2018; Waite et al. 2017).

Another major theme in investigations of the deep subsurface biosphere has been an emerging understanding that the geochemical, geological and isotopic parameters defining the environmental context for subsurface life, the subsurface "landscape," is a powerful and essential framework for deciphering the controls on microbial communities, distribution and function. Unfortunately such "metadata" has arguably too often been collated after the main microbiological investigations were complete. This study highlights the power of a strategic and integrated approach more akin to that used for the astrobiological exploration of other planets, for instance of Mars. Specifically, we highlight the advantages of defining the recharge and geochemical history of the fluids and geological environment at the outset of a microbiological investigation in addition to the relevant nutrients, electron donors, and electron acceptors that might sustain habitability in the subsurface. For example, direct groundwater dating tools such as ^{3}H and ^{14}C are relatively underused to date in subsurface microbiological investigations, and yet are helpful for defining subsurface environments that are still in recent connection with the surface hydrogeologic cycle via recharge (e.g., Borgonie et al. 2015). At the other end of the spectrum, environments isolated from the surface photosphere on geologic timescales, where mixing with recharging surface groundwaters is negligible, can be identified via conservative noble gas tracers and via ^{18}O and ^{2}H analysis of water (Holland et al. 2013; Li et al. 2016; Lippmann-Pipke et al. 2011). These tools can be combined to quantitatively define the timing and extent of mixing between surface and subsurface biomes, or the degree and timing of isolation and sequestration from the surface photosphere. If integrated in the initial phases of subsurface microbiological investigation, such a "Follow the Water" approach using hydrogeochemical tools can define target environments, constrain potential contamination end-members, and allow hypothesis-driven, scientific exploration of the subsurface. This study provides a model for such a hydrogeologically and geochemically constrained approach in one of the world's deepest observatories for investigation of crustal fluids and deep life, along with the first lines of evidence for extant subsurface microbial life in these fracture fluids.

Subsurface scientific observatories of the deep earth

This study focuses on the continental crust, and specifically the Precambrian rocks between ~600 Ma and ~4 Ga in age that represent >72% of the continental lithosphere by surface area (Goodwin 1996; Sherwood Lollar et al. 2014). Several scientific "windows into the continental subsurface" have been developed to address this knowledge gap through major international collaborations. Subsurface laboratories in Sweden, USA, Canada, Finland, UK, France, Japan, and Switzerland have been established (see reviews by Itävaara et al. 2011; Osburn et al. 2014; Sherwood Lollar 2010; Schrenk et al. 2013). The Kidd Creek Observatory is located at 2.4 km below surface in a mine operating to 3 km depth in the 2.7 billion year old rocks of the Canadian Shield near Timmins, Ontario, Canada (Warr et al. 2018). The loci of scientific investigations for subsurface fluids since the early 1990s (Doig et al. 1995; Sherwood Lollar et al. 2002), Kidd Creek hosts a dedicated observatory at the 2.4 km level, in continuous operation since 2008. Routinely monitored for fluid geochemistry for almost a decade, the fluids continuously discharging there represent to our knowledge, the longest time series investigation of subsurface fluids available for the scientific community at such a profound depth. From this location, studies of dissolved gases (Sherwood Lollar et al. 2002, 2006; Young et al. 2017), noble gas residence times (Holland et al. 2013; Warr et al. 2018), and habitability studies (Li et al. 2016) have all been conducted. The observatory is currently the focus of a long-term international collaboration whereby four separate teams of microbiologists have collected samples for culture-based, genomic, and metagenomic analyses and, once complete, results will be compared between the various teams and methodologies. This paper represents the first results from this long-term interdisciplinary initiative at Kidd Creek. The goals of this paper are twofold – first to define the key hydrogeochemical parameters that inform the history of naturally occurring fracture fluids at the site (and by comparison and contrast, the contamination end-member represented by the mine service water), and second to provide the first lines of evidence for extant visible and cultivable microbial life at this location.

Rationale and scope for this study

Samples were collected for this study from two boreholes naturally discharging fracture water (FW) under artesian conditions. Both boreholes (FW12261 and FW12299) have been steadily flowing at rates of tens to hundreds of mL/min since initially drilled in 2007. As noted, these systems provide the world's deepest long-term observatory in Precambrian crystalline rock settings, with continuous geochemical sampling since 2009. As such they are a unique scientific resource, even if not originally drilled for scientific purposes (and, hence, having had no opportunity to apply techniques such as tracer injection during drilling). Even in such disturbed environments, steps to control for contamination during sample collection, and the careful use of environmental controls to monitor for contamination, can be successfully applied. As an essential environmental control in the study, drilling fluids (at this site consisting of recirculated surface water from a local lake – and referred to as "service water" SW) were subjected to the same geochemical, isotopic, and microbiological investigation as the fracture fluids (FW). These data serve as the basis for a comparison

and contrast of putative indigenous microbiology signatures to those of the potential contamination end-member, and is an established approach for differentiating indigenous signals from contamination-related conditions and microbial communities in the subsurface (Kieft et al. 2007; Lin et al. 2006; Santelli et al. 2010). In addition, geochemical and isotopic parameters were used to demonstrate that no detectable trace of drilling fluid contamination remains, as has been done in in subsurface observatories elsewhere (Orcutt et al. 2011; Osburn et al. 2014).

Two fracture waters (FW12299 and FW12261) were selected for geochemical and isotopic investigation in this study. Borehole 12299 has, since 2012, been the focus of a dynamic experiment monitoring recovery of *in situ* conditions analogous to marine CORK experiments (Circulation Obviation Retrofit Kits) (Cowen et al. 2003; Nakagawa et al. 2006) wherein recovery of borehole conditions, and isolation of the borehole by a packer device, allows investigation of the *in situ* geochemistry and microbial community (as has been done in marine settings by Orcutt et al. 2011 among others). In contrast, borehole 12261, located in the same area of the mine as 12299, has remained unpackered, although constant flow of 10–100 mL/min serves as an effective hydrogeologic barrier to any contamination by ensuring the borehole is continuously flushed with fracture water. It is a logical inference that such an open system may represent an intermediate condition between FW12299 and service water (SW), as the flowing anaerobic fracture waters are exposed to the aerobic environment of the mine at least somewhat at their point of discharge from the borehole.

Overall, this study provides a geochemical and isotopic assessment of the contamination fluid end-member in the mine subsurface (SW), of a continually discharging open fracture water system (12261), and of an artificially packered "response and recovery" fracture water end-member (12299). This work thereby provides essential insight into the geochemical and isotopic composition of the fluids defining the deep surface habitable environment that is the focus of this first paper, as well as the focus of the on-going long-term international collaborative investigations. The paper establishes the hydrogeochemical setting – emphasizing the nature of the fracture water discharging from these two boreholes, as well as characterization of the potential contamination end-member (SW) and identifies the key features that distinguish these fluids and hence that serve as the framework for evaluating contamination for this and future studies. In addition, this paper contains the first lines of evidence for extant microbial life in this system based on cell count results for all three systems, and on the Most Probable Number culture-based results for FW12261 and for the SW.

Materials and methods

Geologic setting

Kidd Creek Mine, Timmins, Ontario, is located 24 km north of the town of Timmins, Ontario, Canada (Figure 1) within the Kidd-Munro assemblage of the Southern Volcanic Zone of the Superior Province of the Canadian Shield (Bleeker et al. 1999). The Kidd-Munro assemblage consists of a series of steeply dipping interlayered felsic, mafic, ultramafic and metasedimentary deposits and forms part of the Abitibi greenstone belt. The deepest base metal mine in North America, this Cu–Ag–Zn deposit is a stratiform Volcanogenic Massive Sulfide (VMS) deposit of 2.7 Ga age (Thurston et al. 2008). Ore deposition was triggered by episodic massive hydrothermal vent activity as a result of silica and metal-rich hydrothermal fluid circulation below the seafloor. Above the stringer ore deposits lie banded and massive sulfide ores initially deposited as inorganic precipitates formed where metal-rich hydrothermal solutions mixed with seawater in a system analogous to modern day "black smokers." During intermittent periods of volcanic quiescence, proximal seafloor sediments accumulated forming argillite to chert carbonaceous horizons within the assemblage, the latter forming graphite-rich horizons. Following deposition of the Kidd-Munro assemblage, the entire formation was metamorphosed to greenschist facies during the last major regional metamorphic event at 2.67–2.69 Ga. The last major hydrothermal event in the Timmins area was at 2.64 Ga, followed by low-grade metamorphic hydrothermal events with peak temperatures of between 300 °C and ~220 °C at 2.64 Ga (Bleeker et al. 1999; Smith et al. 1993). The system has been continuously cooling since that time with estimated temperatures below 100 °C for the past two billion years (Li et al. 2016).

Sampling protocols and controls for contamination

In a recent publication on lessons learned arising from the Census for Deep Life decadal study, Sheik et al. (2018) made powerful suggestions for future studies to improve community best practices for obtaining samples for microbiological investigation, especially in subsurface systems challenged by low biomass. They point out that opportunities to control many aspects of sample access, in particular scientifically controlled aseptic drilling, are often limited. This requires the community to develop approaches to maximize information and sample opportunities even from less than ideal environments (Sheik et al. 2018). Following this approach, all procedures in this study adhered to the following steps:

1. Contamination prevention by sterilization of all sample collection apparatus and procedures during collection of fracture and service waters.
2. Collection of environmental controls by conducting the geochemical, isotopic, and microbiological analyses on the "service water" (water used during mining activity and drilling) to determine the background microbial community and geochemistry of those fluids.
3. Confirmation that no service water contamination remains in the targeted fracture waters from which microbiology samples were collected (via geochemical and isotopic analysis of the fracture waters as well as service water).

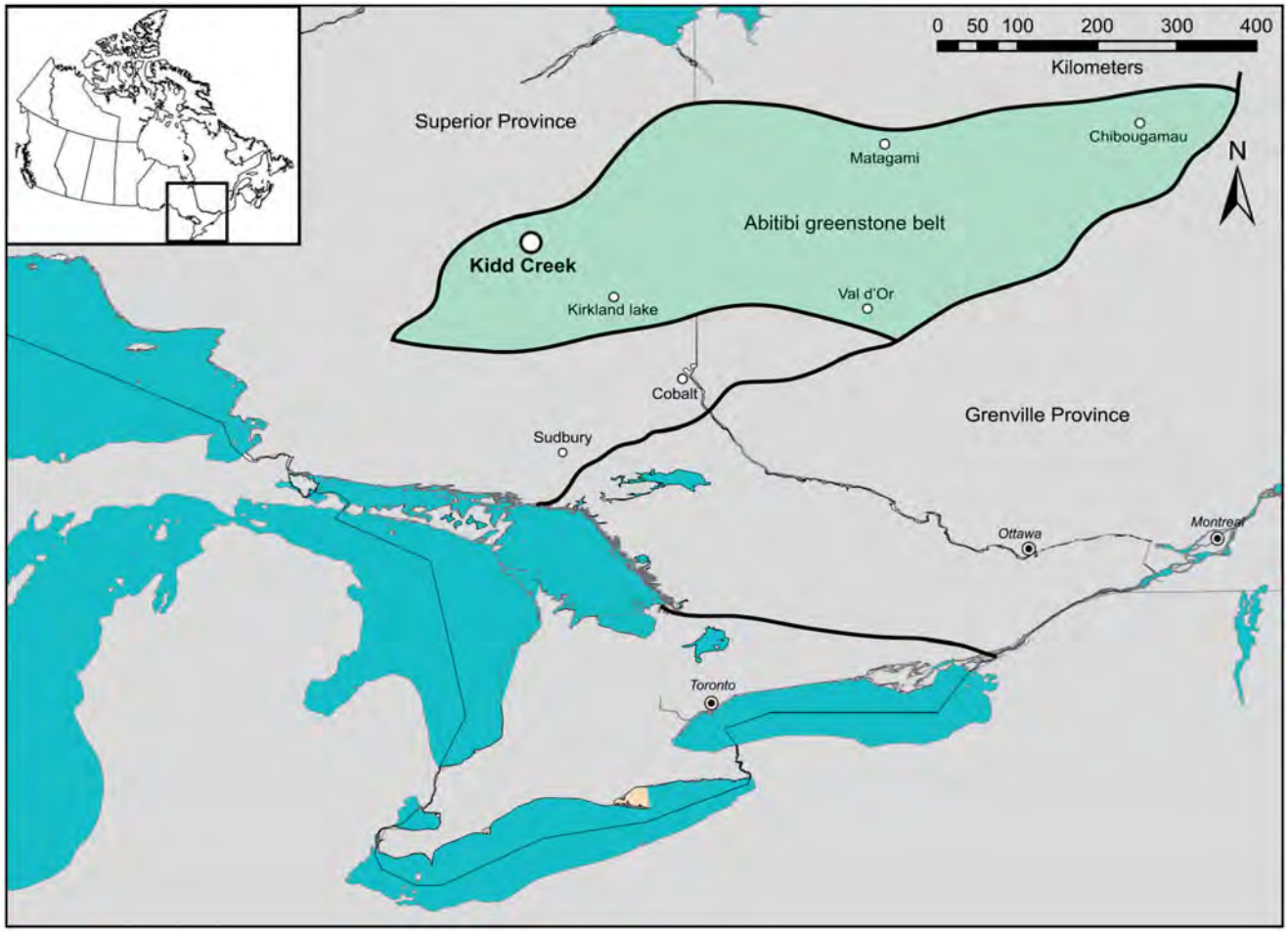

Figure 1. Location map of Kidd Creek in Timmins, Ontario, Canada, in the Abitibi greenstone belt of the Superior Province of the Canadian Shield in crystalline rocks of ~2.7 billion year age. Latitude and Longitude of Kidd Creek Observatory, located at 2.4 km depth below surface is 48° 41′ 24″ North, 81° 22′ 0″ West. Geologic schematic after Thurston et al. (2008).

Mining operations at Kidd Creek involve lateral coring via multiple boreholes at each level as described in detail in Li et al. (2016). Exploration boreholes frequently intersect pockets of fracture fluids trapped within the host rock. Once pierced, fluids from these pockets have been observed to flow over prolonged time periods. Flow of the anaerobic fracture fluids from 12299 and 12261 has been constant since their drilling in 2007 – between 10 and 300 mL/minute – a factor that also contributes to contamination control as the fractures remain well flushed at all times. In addition, at 12299 borehole, a sterile stainless steel manifold which had been previously combusted at 400 °C for 8 h and autoclaved, was connected to the borehole casing as a means of excluding mine air and other contaminants (analogous to a CORK system and described fully in Magnabosco et al. 2016). The main valve and four side valves were opened to let the fracture water that was under natural high pressure flow for several minutes. This process flushed out any water that might have been oxygenated during the initial contact with mine air, and also flushed air out of the sterile manifold. Autoclaved sampling tubes that were subsequently connected to the manifold were also flushed in a similar manner immediately after installation. This manifold allows for the attachment of airtight tubing and filters for sampling for cell counts, and chemical and isotopic analysis of the fracture fluids from 12299.

To obtain fracture water samples for geochemistry, cell counts, and MPNs from borehole 12261, once again all sampling equipment was sterilized in the laboratory and remained sterile until immediately prior to deployment at the borehole. In the mine, narrow autoclaved sampling tubes of about 0.7 m in length were equipped with a sterile disposable 60 mL syringe to insert into the borehole below the water surface to avoid the interface where anaerobic fluids discharge to the aerobic mine environment. Water withdrawn into the syringe from 0.7 m downhole was immediately transferred to pre-sterilized 60 mL serum vials, pre-evacuated to $<5 \times 10^{-3}$ atm. Vials were pre-sealed with Bellco blue butyl stoppers and aluminum crimp seals also pre-sterilized and pre-treated after the method of Ward et al. (2004). For the MPN study this was repeated for 6 vials each for the fracture water and service water. All samples were collected and kept in sterile conditions until they could be added to vials of growth media under anaerobic conditions in the laboratory (within 48 h of collection). Water and gas samples were collected from all fracture

fluids following the methods of Ward et al. (2004) and Warr et al. (2018). All samples were stored under cool temperatures (approximately 4 °C until analysis).

Geochemical measurements

Temperature and pH were measured with hand-held probes (Hanna Instruments, Woonsocket, RI, or Extech Instruments, Nashua, NH). Hydrogen and oxygen isotopic compositions of water samples were determined at the Environmental Isotope Laboratory at the University of Waterloo after the methods of Ward et al. (2004). Errors for individual measurements are ±0.2 and ±0.8 ‰ for $\delta^{18}O_{H2O}$ and $\delta^{2}H_{H2O}$ respectively (Table 1). The anion and cation samples were analyzed by Activation Laboratories Ltd. (ISO/IEC 17025 certified). The anion content of the samples was measured using a DIONEX DX-120 Ion Chromatography System (Ion Chromatography) and their counterpart cation samples were analyzed using Spectro Cirros (ICP-OES). Accuracy of these analyses was confirmed with a charge balance error of less than 5% for all samples and are stated for each sample in Table 2. Methods for analysis of DIC, formate, and acetate were previously published in McDermott et al. (2015). Compositional analysis of gas samples (Table 3) were all performed at the Stable Isotope Laboratory at the University of Toronto, after the methods outlined in Ward et al. (2004) and Sherwood Lollar et al. (2006). All compositional analyses were run in triplicate and mean values are reported. Uncertainty is ±5% by volume.

Table 1. Isotope $\delta^{18}O$ and $\delta^{2}H$ data from the Kidd Creek fracture waters (FW) 12299, 12261, and service water (SW) from the 2.4 km level of the observatory.

Water isotopes			
Sample	FW 12299	FW 12261	Service water (SW)
BH completion date	29 May 2007	17 April 2007	–
Sampling date	12 July 2016	12 July 2016	12 July 2016
$\delta^{18}O_{(H2O)}$ ‰	−12.7	−12.7	−12.6
$\delta^{2}H_{(H2O)}$ ‰	−34.0	−33.5	−91.1

BH completion date refers to the date on which the borehole was drilled.

Cell counts

Cell count samples were collected following the methods of Decoster et al. (2010), by directly filling a 500 mL sterile plastic bottles (Fisher Scientific, Waltham, MA) preloaded with 40 mL of 25% glutaraldehyde (Fisher Scientific# 02957-1, Waltham, MA). Samples were collected in triplicate and stored refrigerated (4 °C) until shipment to Northwestern University for counting. Fluids containing free cells were filtered via 0.2 µM black polycarbonate filters (Whatman #09-800-911). Sample volumes were 10 mL for 12261, 30–60 mL for 12299, and 1 mL for SW. Filtered cells were stained with

Table 3. Gas composition data from the Kidd Creek fracture waters (FW) 12299 and 12261.

Gas compositions (in volume %)		
Sample	FW 12299	FW 12261
BH completion date	29 May 2007	17 April 2007
Sampling date	12 July 2016	12 July 2016
He	2.43	2.28
Ar	0.35	0.39
H_2	3.63	3.07
N_2	13.5	21.7
CH_4	71.9	64.6
C_2H_6	6.97	6.26
C_3H_8	0.93	0.91
i-C_4H_{10}	0.08	0.46
n-C_4H_{10}	0.17	0.23
i-C_5H_{12}	0.04	0.11
n-C_5H_{12}	0.03	<0.05

Service water from the 2.4 km level had dissolved gases less than the detection limit (<d.l). BH completion date refers to the date on which the borehole was drilled.

Table 2. Geochemistry data for major cations and anions from fracture waters (FW) 12299 and 12261, and from service water (SW) from the 2.4 km level.

Geochemical compositions (in mol/L)			
Sample	FW12299	FW12261	Service water (SW)
BH completion date	29 May 2007	17 April 2007	–
Sampling date	12 July 2016	12 July 2016	12 July 2016
Temperature (°C)	25.3	26.0	24[b]
pH	6.5	6.5	7.6[b]
Na^+ (mol/L)	6.5E − 01	6.9E − 01	1.3E − 02
Total Fe (mol/L)	3.8E − 04	4.3E − 04	<3.6E − 05
K^+ (mol/L)	2.7E − 03	2.6E − 03	1.1E − 03
Mg^{2+} (mol/L)	8.8E − 02	7.7E − 02	4.2E − 03
Ca^{2+} (mol/L)	1.3E + 00	1.5E + 00	1.0E − 02
Cl^- (mol/L)	3.5E + 00	4.0E + 00	6.1E − 03
Br^- (mol/L)	2.4E − 02	2.8E − 02	4.3E − 05
NO_3^- (mol/L)	<3.2E − 04	<3.2E − 04	4.1E − 04
NO_2^- (mol/L)	<4.3E − 04	<4.3E − 04	<2.2E − 06
HPO_4^{2-} (mol/L)	<4.2E − 04	<4.2E − 04	<2.1E − 06
SO_4^{2-} (mol/L)	6.2E − 04	6.2E − 04	1.8E − 02
DIC (mol/L)	5.7E − 05[a]	NA	1.4E − 03[a]
Formate (mol/L)	5.5E − 04[a]	NA	7.7E − 05[a]
Acetate (mol/L)	1.4E − 03[a]	NA	<3E − 05[a]
Total salinity (mol/L)	5.5E + 00	6.2E + 00	5.3E − 02
TDS (g/L)	192	220	2.85
Charge Balance	2.2 %	3.0 %	0.7 %

NA and BD indicate sample not analyzed, and sample below detection limit, accordingly.
[a]Sample collected from a previous field trip.
[b]Historical levels of T and pH for service water from the monitoring period 2009 to 2016. TDS: total dissolved solids.

Table 4. Cell count results from the Kidd Creek fracture water FW 12261 (in triplicate), FW 12299 (in duplicate), and service water (SW) (in duplicate) from the 2.4 km level of the mine.

Samples	Cell density (cells/mL)
12261 – 1	7.7×10^4
12261 – 2	6.2×10^4
12261 – 3	1.9×10^4
12299 – 1	1.2×10^3
12299 – 2	2.2×10^3
SW – 1	3.6×10^5
SW – 2	5.2×10^5

DAPI (1 ug/mL, MP biomedicals cat #157574) for 10 min prior to cell enumeration. Cells were imaged on a Zeiss Axioimager M2 Epifluorescence Microscope and ZEN imaging software. Cells were counted manually on a reference grid, counting no less than 10 grids, for a total of no less than 300 cells. Final cell densities were calculated from the known area of the filter, dilution from fixative, and volume of original sample fluid. Laboratory blanks of fixed MilliQ were 2 orders of magnitude lower than samples. Only those cells that were visible in the field of view were counted with no adjustments for cells obscured by sediment particles. The results (Table 4) are, therefore, minimum cell density estimates but nonetheless provide a better estimate of total cell counts than MPN responses (which inherently embed the potential for false negatives due to the limits of culturing indigenous microorganisms under laboratory culture conditions).

Media and culture tube preparations for most probable number analysis

The media in the MPN culture vials were set up to enrich for the anaerobic metabolisms as shown in Table 5. Once inoculations were complete, samples were monitored for 76 d to determine whether there was a positive growth response for each assay. Each vial had sets of replicates and controls, and each replicate used three dilutions: 10×, 100×, and 1000× (Table 6) based on anticipated low biomass levels ($\sim 10^3$) estimated for such systems 2–3 km below surface (Li et al. 2016; Lin et al. 2006). Setting up the vials in this way allows a statistical method to be employed to calculate the number of cells that were present in the original sample, known as the Most Probable Number (MPN) method. These methods are based on Oblinger and Koburger (1975) and Pedersen (2000) and have previously been successfully applied in a similar study by Telling et al. (2018).

The stock media was produced in one liter batches to yield aqueous concentrations for the media equivalent to the fracture water geochemistries in Table 2. The pH of the media mix was then adjusted to ~6 and is referred to as "Stock A." Once Stock A was prepared, a trace mineral stock solution (MM3), and trace vitamins stock solution (MM7) were added after standard laboratory practice (Telling et al. 2018). MM3 is based on the following recipe: H_3BO_3 (0.3 g), ZnCl (0.1 g), $Na_2MoO_42(H_2O)$ (0.1 g), $NiCl_26(H_2O)$ (0.75 g), $MnCl_24(H_2O)$ (1.0 g), $CuCl_22(H_2O)$ (0.1 g), $CoCl_26(H_2O)$ (1.5 g), Na_2SeO_3 (0.02 g), and $Al_2(SO_4)_318(H_2O)$ (0.1 g). MM7 is composed of biotin, folic acid (each 0.02 g), riboflavin, thiamine, nicotinic acid, pantothenic acid, *para*-aminobenzoic acid, cyanocobalamin (vitamin B_{12}), thioctic (lipoic) acid (each added in the amount of 0.05 g), pyridoxine HCl (0.1 g), and Coenzyme M (1.0 g) to create a 10,000× concentration stock solution. The pH was adjusted to 7.0 with 2 N NaOH and stored in 1 or 2 mL aliquots frozen until stock MM7 was used. The final MM7 stock was diluted 1/100 before being put into sterile 160 mL serum bottles and sparged with sterile O_2-free N_2(g) for 15 min. Finally, the bottle was sealed with a sterile black butyl rubber stopper and crimped.

A final component of the experimental set-up was MM8, an iron (II) sulfide stock solution that serves as an oxygen scavenger and is composed of $(NH_4)_2Fe(SO_4)_26(H_2O)$ (19.6 g) and $Na_2S9(H_2O)$ (12.0 g) in 500 mL of O_2-free distilled H_2O. The sodium sulfide was added and mixed before adding the ammonium sulfate. The Erlenmeyer flask was then removed to the antechamber of the anaerobic chamber and cycled three times to evacuate the H_2S being formed. The flask was then moved to the main chamber, and allowed to settle for 24 h. After settling, the clear supernatant was decanted, and replaced with a new 500 mL of the O_2-free distilled water. This sequence was repeated 3 more times to remove any free sulfide in the water. On the last wash, the precipitate was re-suspended such that the total volume of solution was 500 mL to obtain the desired concentration of FeS in the final slurry (2 g/L). The final 500 mL of slurry was dispensed into five 160 mL serum bottles, which were sealed and crimped in the anaerobic chamber. These were then removed for autoclaving. The amorphous ferrous sulfide prepared this way was sterile and anaerobic.

For the experimental set-up, 2 mL of MM3 was added per 1 L of stock A. Each 1 L bottle was then deoxygenated with O_2-free N_2 for more than 1 h, then transferred to the anaerobic chamber where 10 mL of MM8 (the oxygen scavenger) was added and the stock bottle sealed. The bottle and contents were then removed from the glovebox, and autoclaved to ensure all components of the medium were sterilized. As MM7 (the trace vitamins media) cannot be autoclaved without it degenerating the vitamins, 1 mL of MM7 was filter-sterilized and then added to the 1 L stock bottle.

Chemglass Life Sciences anaerobic culture tubes (CLS-4209) were used for the enrichment cultures. Tubes were left in the transfer antechamber of the anaerobic chamber under the anaerobic gas mixture over night to ensure degassing was complete, before being introduced to the main chamber. About 9 mL of culture medium were then added to each vial inside the anaerobic chamber. Any additional components (e.g., pre-autoclaved nails or Durham tubes) were added for the appropriate metabolisms, and additions specific to each investigated metabolism were also added (details in Table 5). Table 5 describes all the microbial metabolisms investigated as well as the "signal" used to determine if there was a positive response for this metabolism ("Assay").

Table 5. MPN cultures tubes designed to assay for positive growth responses for a variety of anaerobic metabolisms.

Tested metabolism	Electron donor	Electron acceptor	Additions per 1 L of media	Headspace gas	Assay for positive growth
General fermentative heterotrophs	Glucose, peptone	Glucose, peptone	10 g glucose, 5 g peptone, 0.1 g yeast extract, 2 drops bromocresol purple	CO_2, N_2	Visual: acidification – media turns yellow. Also gas production by floating of Durham tubes
Autotrophic Fe(III)-reducers	H_2	Fe^{3+}	Ferric citrate 12.3g/L (50 mM)	H_2, CO_2, N_2	Visual: positives turn from orange to green to colorless
Autotrophic SO_4^{2-} reducers	H_2	SO_4^{2-}	Sodium sulfate (20 mM), iron nail	H_2, CO_2, N_2	Visual: blackening of iron nail
Autotrophic methanogens/ acetogens	H_2	CO_2	H_2, CO_2, N_2	H_2, CO_2, N_2	GC and/or IC detection: methane, hydrogen, acetate
Heterotrophic Fe(III)-reducers	Acetate, lactate, pyruvate	Fe^{3+}	Ferric citrate (50 mM), sodium acetate (10 mM), sodium lactate (10 mM), sodium pyruvate (10 mM)	CO_2, N_2	Visual: positives turn from orange to green to colorless
Heterotrophic SO_4^{2-} reducers	Acetate, lactate, pyruvate	SO_4^{2-}	Sodium sulfate (20 mM), sodium acetate (10 mM), sodium lactate (10 mM), sodium pyruvate (10 mM), iron nail	CO_2, N_2	Visual: blackening of iron nail
Heterotrophic methanogens	Acetate, methanol	Acetate, methanol	Sodium formate (40 mM), sodium acetate (10 mM), methanol (10 mM)	CO_2, N_2	GC detection: methane
Anaerobic alkane oxidizing SO_4^{2-} reducers	C_{1-4} alkanes	SO_4^{2-}	Sodium sulfate (20 mM), iron nail	CO_2, N_2, C_{1-4} alkanes. Over-pressurize with C_{1-4} alkane mix to 1.8 atm after autoclaving	Visual: blackening of iron nail. Highest dilution positives can be assayed for SO_4^{2-} depletion (IC) and C_{1-4} alkanes (GC)
Anaerobic alkane oxidizing Fe(III) reducers	C_{1-4} alkanes	Fe^{3+}	Ferric citrate (50 mM)	CO_2, N_2, C_{1-4} alkanes. Over-pressurize with C_{1-4} alkane mix to 1.5 atm after autoclaving	Visual: positives turn from orange to green to colorless. Highest dilution positives can be assayed for C_{1-4} alkanes by GC
Nitrogen fixers	Enzymatic assay	Enzymatic assay	0.2 mL of C_2H_2 injected into the headspace (PC_2H_2 = 1 kPa)	C_2H_2, CO_2, N_2	GC detection: ethylene

Details of each assay preparation, headspace gas composition, and positive growth indicator after the method of Telling et al. (2018).

Table 6. 1, 2, and 3 are replicates of the same metabolism.

FW12261			Service water (SW)		
1A	2A	3A	1A	2A	3A
1B	2B	3B	1B	2B	3B
1C	2C	3C	1C	2C	3C
1D	2D	3D	1D	2D	3D

Lighter shading represents 10× dilution from the source material (where darkest shading represents 10^{-1}, and the lightest shading represents a dilution of 10^{-3}). The white shading represents the controls (filtered source water in media). Each metabolism therefore has 24 tubes associated with it – for a total of 240 tubes in the experiments overall.

MPN inoculations and dilutions

For fracture fluid FW 12261 and for the service water (SW), in each case, 1 mL of sample fluid was added to the 9 mL prepared culture media tubes described above, for each of 10 metabolisms tested. The culture tubes were then sealed with Bellco Blue butyl stoppers crimped sealed with an aluminum cap (after the method of Telling et al. 2018; Ward et al. 2004). There were three replicates for each tube, which involved three subsequent dilutions from 10^{-1} to 10^{-3} for each setup. For dilutions, a 1 mL syringe and 21 gauge needles were used to pierce the blue butyl stoppers. About 1 mL was taken from Vial A and injected into the next dilution vial using the same technique as for the first dilution. This diluted the sample 10× from the previous dilution (to 10^{-2} from the original sample). This process was repeated for the third and final dilution (resulting in 10^{-3} from the original sample). The needle was not allowed to touch the liquid or the walls to prevent mixing lower dilution samples with more diluted samples. A new sterile syringe and a new sterile needle were used for each step. Controls were prepared by setting up tubes identical to the FW and SW sample replicates but for which the source waters and culture medium were first filtered through a 0.2-μm filter. Table 6 provides a visualization of the experimental set-up and number and distribution of MPN tubes and controls. Each metabolism had 24 tubes associated with it – for a total of 240 tubes in the experiments overall.

The responses in the MPN tubes were tracked and scored based on a positive "yes" or negative response "no" scale as per standard MPN methods (Oblinger and Koburger 1975; Pedersen 2000). The Most Probable Number (MPN) method is a statistical method that provides quantitative cell count approximations based on whether a certain vial with a given concentration of sample will have a response during cultivation experiments of the type described above (Oblinger and Koburger 1975; Pedersen et al. 2014). The approach is based on serial dilution tests to measure the concentration of target microbial metabolism and is particularly useful for low concentration organisms and those environmental samples in which particulate matter may interfere with other counting techniques (Blodgett 2010). The MPN approach also

Table 7. Viable most probable numbers of microbial cells in fracture water (FW) and service water (SW).

Tested metabolism	Time points (days)	SW (cells mL^{-1})	FW 12261 (cells mL^{-1})
Heterotrophic SO_4^{2-} reducers	13	240	43
	32	>1100	43
	76	>1100	93
Autotrophic SO_4^{2-} reducers	13	3.6	23
	32	>1100	>1100
	76	>1100	>1100
Alkane-oxidizing SO_4^{2-} reducers	13	>1100	>1100
	32	>1100	>1100
	76	>1100	>1100
General fermentative heterotrophs	All	<3	<3
Autotrophic Fe(III) – reducers	All	<3	<3
Heterotrophic Fe(III) – reducers	All	<3	<3
Autotrophic methanogens/acetogens	All	<3	<3
Heterotrophic methanogens	All	<3	<3
Anaerobic alkane-oxidizing Fe(III) reducers	All	<3	<3
Nitrogen fixers	All	<3	<3

provides a complementary and alternative method of determining not only the presence of extant life ("who is there") but "who is active." This complementary approach is particularly useful in extreme environments where low biomass, high salinity, and high particulate content in fracture fluids make standard molecular methods of DNA extraction more of a challenge. MPN response is based on a positive/negative dichotomy of possible results from the test and is known as incidence data. The potential for false negatives is inherent due to the possible lack of response related to stress imposed by the experimental context. The statistical method is represented by the following equation which is solved by iteration (Blodgett 2010):

$$\sum_{j-1}^{k} (g_j m_j)/\left(1 - \exp\left(-\lambda \mathrm{m}_j\right)\right) = \sum_{j-1}^{k} t_j m_j \qquad (1)$$

where K denotes the number of dilutions, g_j denotes the number of positive (or growth) tubes in the jth dilution, m_j denotes the amount of the original sample put in each tube in the jth dilution, and t_j denotes the number of tubes in the jth dilution. MPNs typically use three serial dilutions and a decimal series (each dilution has one tenth as much of the sample as the previous dilution) (Table 6) and this approach was used in this study. Upper and lower detection limits were 1100 cells/mL and 3 cells/mL, respectively (after the method of Blodgett 2010) (Table 7). The upper limit simply means the dilution method cannot distinguish between a response >1100 cells/mL (all responses > than this value count as a maximum positive response for the relevant metabolism). Cell counts undertaken in this study (Table 4), therefore, provide a more quantitative estimate of the total cells, while the MPN results identify the dominant metabolic responses.

Results and discussion

"Follow the Water" has been a core concept applied in planetary sciences and the astrobiological related exploration of Mars. Arguably it is a concept that has been less consistently integrated into investigations of subsurface life on

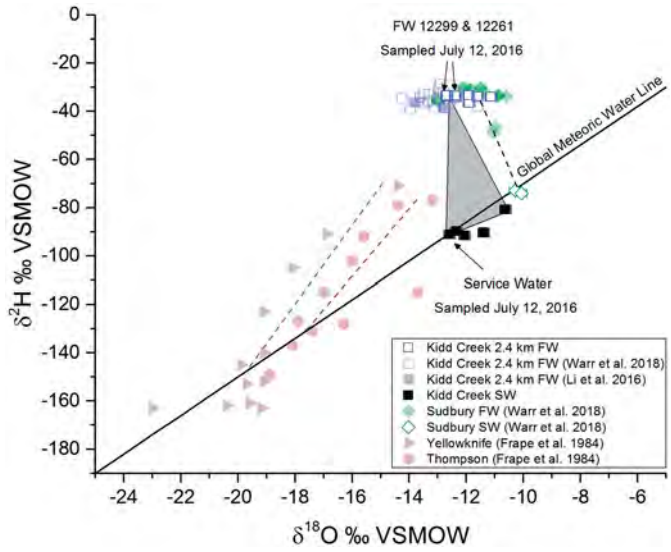

Figure 2. The $\delta^{18}O$ and $\delta^{2}H$ signatures for fracture waters from this study (open blue squares) and for service water (black squares) sourced from a local surface lake, plotted with respect to the Global Meteoric Water Line (GMWL) from Craig (1961). Additional $\delta^{18}O$ and $\delta^{2}H$ values shown for Kidd Creek (KC) (unpublished, and from Li et al. 2016; Warr et al. 2018) and for additional sites on the Canadian Shield: Sudbury (from Warr et al. 2018), Yellowknife, and Thompson (both from Frape et al. 1984). Hatched lines show approximate mixing lines between service waters (on GMWL) and fracture waters for Sudbury, Thompson and Yellowknife. More extensive sampling of Kidd Creek service water allows identification of possible mixing space between service water and fracture waters at the Kidd Creek Observatory (shaded triangle). This data demonstrates there is no evidence of mixing with mine service waters impacting the fracture waters 12299 and 12261 in this study. Error bars are smaller than the plotted symbols.

Earth to date. While intuitively simple – life requires water to survive – paradoxically a thorough understanding of the hydrogeologic environment is sometimes an afterthought in subsurface microbiology – relegated to "metadata" incorporated at the later stages of investigation and interpretation. Yet it is clear that certain key hydrogeochemical measurements, integrated into the early stages of an investigation, may serve as critical guides to design and execute sampling strategies as well as providing a vital contextual framework for interpretation. One somewhat underdeveloped tool in the subsurface microbiology arsenal is $\delta^{18}O$ and $\delta^{2}H$. With the advantages of being inexpensive, simple to collect, and routinely available both in research and commercial laboratories worldwide, we demonstrate here why $\delta^{18}O$ and $\delta^{2}H$ measurements should be a much more comprehensively applied first line investigative tool for subsurface microbiology.

Figure 2 demonstrates the global pattern of $\delta^{18}O$ and $\delta^{2}H$ values known as the Global Meteoric Water Line (GMWL) (Craig 1961). Worldwide, waters of "meteoric" origin fall along this classic global trend with a canonical slope of 8 where "meteoric" refers to water that has been in "contact with the atmosphere" or more specifically, in the case of meteoric groundwater, whose $\delta^{18}O$ and $\delta^{2}H$ values still reflect the conditions associated with their recharge from surface. As recharge is largely an isotopically conservative process, groundwaters that have recharged in the recent geologic past (tens to thousands of years) continue to reflect their meteoric origin via signatures that still fall along the

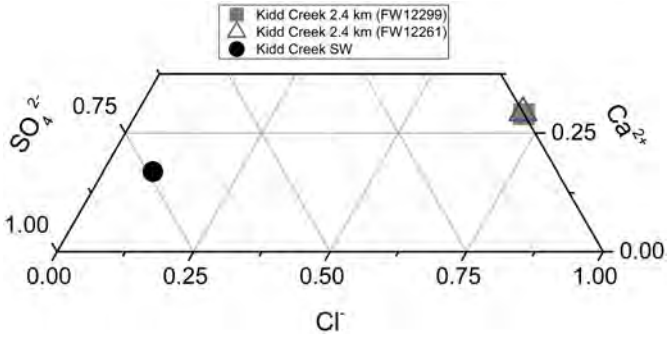

Figure 3. Ternary plot of major geochemical ions (Ca^{2+}, Cl^{-}, SO_4^{2-}) demonstrates the similar geochemical features of the two fracture waters (12299 and 12261) and the distinct differences in the geochemistry of the service water. Along with the isotopic and geochemical details in Tables 1 and 2, these data confirm there is no mixing with service water impacting the two fracture fluids 12299 and 12261.

GMWL line. In contrast, in crystalline rocks of Precambrian age throughout the world, fracture fluids typically lie above the GMWL – attributed to the effects of a variety of low temperature water–rock reactions (WRI) (Frape et al. 1984; Li et al. 2016; Onstott et al. 2006). While $\delta^{18}O$ and $\delta^{2}H$ signatures are not a dating tool, as the deviation above the GMWL increases with the extent of WRI, typically the further above the line, the older the fluid residence time – and so deviation above the GMWL can be used to some degree as an initial proxy for residence time (Heard et al. 2018; Lippmann-Pipke et al. 2011; Ward et al. 2004). In all cases, mixing between fluids of different origin (meteoric and non-meteoric) can produce mixing trends that reflect the relative contribution of each end-member to the groundwater system under-investigation.

Geochemistry and isotopic signatures of fracture waters and service water

Figure 2 shows the $\delta^{18}O$ and $\delta^{2}H$ values for fluids under investigation in this study – FW12261, FW12299, and service water (SW) (Table 1), compared to values from the literature for other sites on the Canadian Shield. The Kidd Creek service water sample from this study falls along the GMWL, consistent with the fact that mine service waters are of surface origin drawn from a lake near the property, pumped to depth and recirculated for mine operations. Figure 2 demonstrates the range of $\delta^{18}O$ and $\delta^{2}H$ values for the service water used on the 2.4 km level of the mine – and shows the classic signature discussed above for surface lake waters. Specifically, the SW shows a range from values falling directly on the GMWL, to values falling slightly below the line and reflecting a slope of 7 – a typical "lakewater" slope, rather than the GMWL canonical slope of 8. The shaded triangle represents where fracture waters would lie if mixing with, or contamination by the SW end-member is occurring in the fracture waters discharging from the boreholes at Kidd Creek. As an example, Figure 2 shows in green the $\delta^{18}O$ and $\delta^{2}H$ values for SW and FW from a previous study at a mine in Sudbury, Ontario (Warr et al. 2018). In this case, a subset of fracture waters can be identified that are contaminated with mine SW, as they lie in an intermediate position along the hatched mixing line for this site.

In contrast, the samples for both fracture waters at 2.4 km at Kidd Creek, monitored over the past 9 years, are all located far above the GMWL. The Kidd Creek fracture waters all show the elevation above the GMWL characteristic of saline waters and brines from deep Precambrian settings throughout the world. In fact, the fracture waters at Kidd Creek are the most depleted samples with regard to $\delta^{18}O$ and most enriched with regard to $\delta^{2}H$ ever recorded – consistent with the ancient noble gas residence times calculated for these fluids (Holland et al. 2013; Warr et al. 2018). The $\delta^{18}O$ and $\delta^{2}H$ values for 12299 and 12261 on the date of sampling are indicated on Figure 2 and clearly demonstrate the isotopic composition of these fracture waters are distinctly different from those of the SW. None of the FW in this study falls within the shaded wedge that would indicate an impact due to mixing with, or a remnant of service water used during drilling. The large amounts of water that have discharged from these boreholes since the time of drilling completion (estimated to be $>1.3 \times 10^{6}$ L, and $>4.3 \times 10^{5}$ L from 12299 and 12261, respectively) have flushed out any contaminating fluid and hence these samples represent indigenous uncontaminated groundwater end-members.

This finding is further supported by the very different geochemistries observed for the FW and SW samples (Tables 2 and 3). The geochemical results demonstrate that in terms of cation and anion chemistry (Table 2 and Figure 3) and dissolved gases (Table 3), the two fracture waters are the same within analytical uncertainty, consistent with their similar $\delta^{18}O$ and $\delta^{2}H$ values. Examination of the core logs for these two boreholes in fact show that the boreholes are near parallel (beginning at approximately the same point, they diverge by only 0.5 m per meter of borehole length) so that, for instance, at a distance of 100 m length, they remain only 50 m apart. The logs indicate the first 100 m are also the most highly fractured sections of these two boreholes and most likely to be the source of the fluids entering the holes. Given the almost identical isotopic and geochemical chemistry of 12299 and 12261, it is likely that in fact these two boreholes are drawing fluids from the same fracture network (a finding that has also been postulated based on the comparable noble gas compositions of the waters from each borehole published previously by Warr et al. 2018).

Importantly, the geochemical results for the service water are very different from the fracture waters (Table 2 and Figure 3) and demonstrate that the SW end-member, representing the contaminating influence of the mine, is substantially different and readily distinguishable from the indigenous fluids. While the fracture waters are Ca–Na–Cl brines with high levels of bromine and no detectable nitrate, nitrite or phosphate, the service water is considerably less saline, with a total dissolved solids (TDS) value of only 2.9 g/L compared to 192–220 g/L for the FWs. In particular, the service water has notably higher concentrations of nitrate and sulfate compared to the FWs. Overall, the $\delta^{18}O$ and $\delta^{2}H$ values, dissolved gas, and ion chemistry

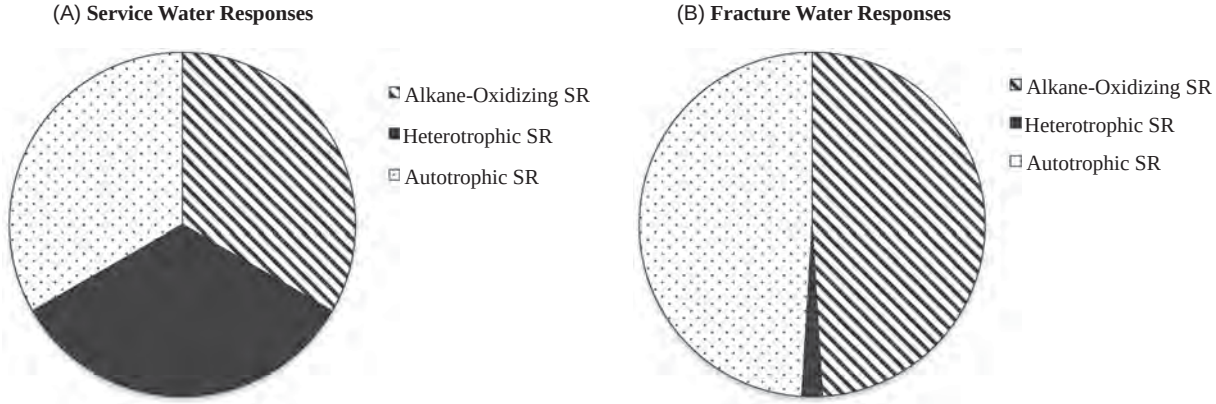

Figure 4. Most Probable Number (MPN) results (in % proportion of total sulfate-reducing metabolism responses), based on the number of responses found in each growth vial for each dilution after 32 d post-inoculation (see text, Table 7) for service water (SW), and for fracture water FW 12261 (A,B), respectively). The upper detection limit for each response is 1100 cell/mL; hence, the cell count results (Table 4) provide the best estimate of total cells/mL, while the MPN results elucidate the dominant metabolic responses. The major differences in response for SW versus FW 12261 are that heterotrophic SRBs are only a minor component of 12261, which is instead dominated by alkane oxidizing and autotrophic SRBs.

demonstrate that while both FW and the SW were collected from the same level of the mine (2.4 km below surface), they represent distinct end-members in terms of geochemistry and isotopic composition. There is no evidence of a contribution of service water to the fracture water samples. This hydrogeological and geochemical information provides essential constraints and context for the microbiological investigations of cell counts and MPNs in this study.

Cell counts identify extant microorganisms

Working in the Witwatersrand Basin, Lin et al. (2006) and Chivian et al. (2008) provided multiple lines of evidence to document the degree to which the fracture waters they investigated 2.8 km below surface in the Mponeng gold mine were cut off from the photosphere. As in this paper, these multiple lines of evidence included $\delta^{18}O$ and $\delta^{2}H$ values, water geochemistry and noble gas-derived residence times that demonstrated the fracture waters in Mponeng were distinct from the service mining water end-member. Biomass indicators, specifically extractable DNA, were several orders of magnitude higher for service water versus the fracture water, consistent with the low cell count densities of 10^3–10^4 typically found in the deep subsurface (Lin et al. 2006). Based on both culture-based, 16s ribosomal DNA, and metagenomics, sulfate-reducing bacteria (SRBs), and in particular, autotrophic hydrogen-utilizing SRBs were demonstrated to dominate the microbial community (Lin et al. 2006; Chivian et al. 2008).

For the samples in this study, cell counts show a similar pattern to that observed in Lin et al. 2006 (Table 4). Specifically, the SW samples contained cell counts of 10^5 cells/mL, an order of magnitude greater than any of those from the fracture waters. In contrast, the FWs had cell counts of 10^3 (12299) to 10^4 cells/ml (12261), comparable to those reported from the Mponeng gold mine in South Africa (Lin et al. 2006), calculated by Li et al. (2016) for Kidd Creek, and characteristic of deep terrestrial microbiomes (Bomberg et al. 2016; McMahon and Parnell 2014).

Most probable number results reveal presence of sulfur-reducing metabolisms

Based on what has been found in deep subsurface sites like Mponeng, and on the indirect evidence from Li et al. (2016) for sulfate-reducing bacteria active in the Kidd Creek fracture waters in the geologic past, a key goal for this study was to determine if sulfate-reducing microbes exist in the fracture waters of Kidd Creek in the present day. Given the anaerobic nature of these fluids (Holland et al. 2013; Li et al. 2016), this study focused on anaerobic microbial metabolisms (Table 7). Only the three sulfate-reducing metabolisms yielded positive responses, although those responses were different for the fracture water versus the service water. For alkane-oxidizing sulfate reducers there was a strong positive MPN response in both fracture water and service water (Figure 4(A,B)). In fact, at 13 d the most probable number of cells for both FW and SW for alkane-oxidizing sulfate reducers was greater than 1100 cells/mL, which represents the upper detection limit for the MPN technique employed in this suite of experiments (Table 7). For both SW and FW, the results indicate a strong positive response from the alkane-oxidizing SRBs throughout the experiments. For the SW, the second major response at 13 d was for heterotrophic sulfate reducers (Table 7). Throughout the experiments, the SW MPNs for this metabolism had also exceeded the detection limit (> 1100 cells/mL), indicating a strong MPN response. In contrast, the MPN response for heterotrophic sulfate reducers for the fracture water (FW) was substantially different. At all time points, the FW only elicited a minor response of 43–93 cells/mL (Table 7). The greatest difference between responses in the service and fracture waters is that the fracture water consistently shows only a very small response for heterotrophic sulfate reducers (Figure 4(B)), while for the SW, there was a substantial response for the heterotrophic sulfate reduction pathway throughout (Figure 4(A)).

In contrast to the SW results, the FW metabolisms are dominated by alkane-oxidizing sulfate reducers and autotrophic sulfate reducers (Figure 4(B)). The positive response for sulfate reduction metabolisms, and especially the

dominance of autotrophic over heterotrophic sulfate-reducers in the FW, is consistent with findings from other subsurface ecosystems at depths of 2–3 km investigated to date where autotrophic metabolisms dominate over heterotrophic metabolisms despite the presence of some labile DOM in the fluids (Kieft et al. 2018; Li et al. 2016; Lin et al. 2006). Given that Li et al. (2016) used naturally occurring sulfur isotope signatures to propose that SRBs must have been present in Kidd Creek fracture waters on geologic timescales, one of the important outcomes of this study is that these results demonstrate sulfate-reducing bacteria continue to exist in the Kidd Creek fracture water in the present day. The combined data of distinct hydrogeologic and isotopic characteristics of the fracture water versus the service water; the significantly lower cell count biomass density in the fracture waters versus the service water; and the differential response in MPNs for sulfate-reducing metabolisms in the two types of fluids; all provide lines of evidence to suggest there is an extant indigenous microbial population in the Kidd Creek fracture waters. The identification of sulfate-reducing organisms in these fluids, both in the geologic past (Li et al. 2016) and in the present day (this study) is an important finding extending our understanding of the deep subsurface biosphere. Understanding when these fracture fluids were colonized by life remains an outstanding question but can begin to be constrained by application of a variety of groundwater dating approaches.

Understanding groundwater residence times

The Kidd Creek Observatory is the site where fracture waters with the longest groundwater residence times ever discovered have been found. Based on the world's highest radiogenic concentrations of the noble gas elements helium, neon, argon and xenon in free fluids, coupled with U, Th, and K contents of the host rock, the linear accumulation method of groundwater dating provides mean residence times for the fracture fluids from the 2.4 km level of 0.9–1.5 billion years (Holland et al. 2013; Warr et al. 2018) for samples collected in 2008–2010. As this discovery dramatically extended our concepts of the timescale on which groundwaters can be preserved in the crust, it is important to understanding these findings in the context of what is meant by groundwater "age." Bethke and Johnson (2008) provided an insightful review – discussing the evolution of the definition of groundwater age from one focusing on "the interval of time that has elapsed since groundwater at a given location in a flow regime entered the subsurface via recharge," to a more quantitative definition that currently prevails and is less dependent on assumptions of 1-dimensional piston flow. Specifically, the definition of groundwater age now prevalent incorporates the concept of "age" as a cumulative property of a water system that reflects the average age of all the various components that have contributed to the system. Hence, a complete model of the residence time of a groundwater system is best achieved by applying multiple lines of evidence including dating systems that can constrain both the "youngest" components and the "oldest" contributions to the system (in addition to critical parameters such as porosity and hydraulic conductivity estimates and their spatial distribution and scale) (Bethke and Johnson 2008 and references therein).

In the Kidd Creek fracture fluids for instance, while the mean groundwater residence times range from 0.9 to 1.5 Ga, the oldest components can be identified based on ^{129}Xe excesses reflecting interaction with the Archean atmosphere 2.64 billion years ago, and preserved in the ancient fluids (Holland et al. 2013). Identification of the youngest contributions in this system is more challenging, though as demonstrated by the δ^{18}O and δ^{2}H data in this paper, as well as the noble gas data from Holland et al. (2013), a contribution from modern groundwater or atmosphere can be quantitatively ruled out. A key question remains, however, whether the youngest contributions to these fracture waters are from fluids millions of years, or "merely" hundreds of thousands of years old. This question is particularly relevant to the investigation of subsurface life, as conceivably any microbial life in these fluids could be as young as the youngest contributing fluid. Groundwater dating tools using ^{81}Kr, ^{36}Cl, and ^{129}I (with half-lives of 229,000, 301,000, and 1,570,000 years, respectively) are being applied to this system as a step in constraining this aspect but will require careful characterization of the background in these U- and Th-rich crystalline rocks where additional subsurface sources of ^{36}Cl (via neutron capture by stable ^{35}Cl; Lehmann et al. 1993) in these Ca–Cl-rich brines; and of ^{81}Kr and ^{129}I (via subsurface fissiogenic production (Andrews et al. 1989; Purtschert et al. 2017) make such applications non-routine.

Constraining the timing of subsurface ecosystems

A conservative time limit for the habitability of these systems is the time period when this geologic setting last exceeded the known thermal limits to life. These host rocks would have been sterilized by the last major regional metamorphic event at 2.67–2.69 Ga (Bleeker et al. 1999; Thurston et al. 2008). Hence, a thermal regime compatible with life was possible any time in the past two billion years once the rocks cooled to estimated temperatures below 100 °C (Li et al. 2016). As noted above, however, life could likely be as young as the youngest fluid contribution and hence recent results by Warr et al. (2018) are particularly relevant. By monitoring the temporal changes in noble gas-derived residence times for the same suite of fracture waters as the original Holland et al. (2013) study, the 2018 study documented shifts in mean residence time from $>$ 1 billion years, to values between 149 and 658 million years, consistent with expected changes in the age distribution of fluids feeding the fractures as they drain. Over time, the total fracture fluid receives a decreasing proportion of the oldest components and the younger fluids make up a larger proportion of the total fluid, resulting in a reduced mean residence time (Warr et al. 2018). This temporal monitoring suggests that some of the fracture fluids feeding the Kidd Creek systems might be only as old as 150–650 million years. In the Witwatersrand Basin, fluids with a similar

range of residence times (on the order of hundreds of millions of years; Heard et al. 2018; Lippmann et al. 2003; Lippmann-Pipke et al. 2011) have been shown to host indigenous microbial ecosystems (Chivian et al. 2008; Lin et al. 2006; Lau et al. 2016; Ward et al. 2004) dominated by hydrogen utilizing sulfate reducers. The identification of extant microorganisms in these deep ancient fluids on the Canadian Shield suggests that such isolated microbial ecosystems may be common in the globally distributed crystalline rocks of the Precambrian Shields that had been previously shown to be a vast habitable zone of the continental lithosphere (Sherwood Lollar et al. 2014). This finding extends our understanding of the deep biosphere on Earth and has important implications for the search for extant and extinct life on Mars, and other planets and moons in the solar system (NASEM 2018). The results raise the important question of how long fracture fluids can be stored in the subsurface on geologic timescales and how long either extant microbial ecosystems, or biomarkers of past life, can be preserved (NASEM 2018). As we continue to monitor these fracture fluids, to apply additional methods to constrain the youngest fluid component contributing to these waters, and to integrate results from the genomic and metagenomics samples currently under analysis by the participating teams, we anticipate any variations in the microbiological populations over time for these fracture waters, a comparison of the packered ("corked") 12299 fracture fluid versus the openly flowing system 12261, and comparison to previously characterized deep microbial communities from the Witswatersand Basin and elsewhere, will extend our understanding of deep subsurface life in these ultra-deep and as yet unexplored parts of our planet, and inform our exploration for signs of life elsewhere in the solar system.

Conclusions

Culture-based and non-culture-based analyses have demonstrated that sulfate-reducing organisms are often dominant in deep subsurface ecosystems (Chivian et al. 2008; Lin et al. 2006; Schrenk et al. 2013). Hydrogen-utilizing autotrophic sulfate-reducing bacteria (SRBs) in particular have been identified in microbial ecosystems in deep subsurface environments in the gold mines of the Witwatersrand Basin of South Africa (Onstott 2016). In deep subsurface communities in Fennoscandian bedrock fluids or the Sanford Underground Research Laboratory (SURF) in the former Homestake Gold Mine, South Dakota USA, alkane-oxidizing SRBs were also found, suggested to be utilizing small carbon molecules from serpentinization reactions or organic-rich graphite zones in the host rock (Osburn et al. 2014; Purkamo et al. 2015; Schrenk et al. 2013). For the Kidd Creek deep fracture waters, a previous work on sulfur isotope signatures provided indirect evidence for a longstanding indigenous population of sulfate-reducing bacteria in the fracture fluids (Li et al. 2016). In this study, the combination of cell counts and MPN results, and the distinct differences between the results of the microbiological investigation of the fracture waters versus the mine service waters, provide multiple lines of evidence for the presence of an indigenous population of sulfate-reducing bacteria in the highly saline fracture fluid. The geochemical differences between the fracture and service water at Kidd Creek show that each fluid source has a distinct isotopic and geochemical signature. Hence, this study has provided the foundational data and approach for distinguishing between possible contaminant fluid end-members (service water) and the indigenous fracture fluids of the Kidd Creek Deep Fluid and Deep Life Observatory. The approach provides a best practice example of developing hydrogeochemical parameters to differentiate fluids in complex deep subsurface systems, and for evaluation of potential cross-contamination and mixing using basic geochemistry and isotopic ($\delta^{18}O$ and $\delta^{2}H$) measurements. Together these multiple lines of investigation provide the interpretational framework (chemical, hydrogeologic, and microbiologic) that is essential to the on-going genomic and metagenomics investigations being carried out by multiple international partners at the Observatory. In future work, results from the genomic and metagenomics samples from the Kidd Creek Observatory will help confirm indigeneity and determine the detailed characteristics of the subsurface ecosystem.

Disclosure statement

The authors attest there are no financial interests or benefits arising from the direct applications of this research.

Funding

This study was supported by the Canada Research Chairs program, Natural Sciences and Engineering Research Council of Canada Discovery and Accelerator grants, and additional funding from the Deep Carbon Observatory and Nuclear Waste Management Organisation. M. R. O. and B. S. L. are CIFAR Fellows. Thanks are due to colleagues and partners at Glencore whose efforts and support for the sampling program were invaluable.

ORCID

Garnet S. Lollar http://orcid.org/0000-0001-8206-6828
Oliver Warr http://orcid.org/0000-0001-8240-7979
Jon Telling http://orcid.org/0000-0002-8180-0979
Magdalena R. Osburn http://orcid.org/0000-0001-9180-559X
Barbara Sherwood Lollar http://orcid.org/0000-0001-9758-7095

References

Andrews JN, Davis SN, Fabryka-Martin J, Fontes J-C, Lehmann BE, Loosli HH, Michelot J-L, Moser H, Smith B, Wolf M. 1989. The in situ production of radioisotopes in rock matrices with particular reference to the Stripa granite. Geochim Cosmochim Acta 53(8): 1803–1815.

Bach W, Edwards KJ. 2003. Iron and sulfide oxidation within the basaltic ocean crust: implications for chemolithoautotrophic microbial biomass production. Geochim Cosmochim Acta 67(20):3871–3887.

Bethke CM, Johnson TM. 2008. Groundwater age amd groundwater age dating. Annu Rev Earth Planet Sci 36(1):121–152.

Bleeker W, Parrish RR, Sager-Kinsman A. 1999. A 2.7 Ga komatiite, lois ti tholeiite transition, and inferred proto-arc proto-arc to arc

transition and the geodynamic setting of the Kidd Creek deposit: evidence from precise trace element data. In: Hannington, MD, Barrie, CT, editors. The Giant Kidd Creek Volcanogenic Massive Sulfide Deposit, Western Abitibi Subprovince, Canada, Vol. Economic Geology Monograph 10. Littleton, U.S.A.: Economic Geology Publishing Co., p 43–69.

Blodgett R. 2010. Most Probable Number from Serial Dilutions. U.S. Food and Drug Administration. Bacterial Analytical Manual. Appendix 2.

Bomberg M, Lamminmäki T, Itävaara M. 2016. Microbial communities and their predicted metabolic characteristics in deep fracture groundwaters of the crystalline bedrock at Olkiluoto, Finland. Biogeosci Discuss 13(21):6031–6047.

Bomberg M, Nyyssönen M, Pitkänen P, Lehtinen A, Itävaara M. 2015. Active microbial communities inhabit sulphate-methane interphase in deep bedrock fracture fluids in Olkiluoto, Finland. BioMed Res Int 2015:979530.

Borgonie G, Linage-Alvarez B, Ojo AO, Mundle SOC, Freese LB, Van Rooyen C, Kuloyo O, Albertyn J, Pohl C, Cason ED, et al. 2015. Eukaryotic opportunists rule the deep subsurface biosphere in South Africa. Nat Commun 6(1):8952.

Chivian D, Brodie EL, Alm EJ, Culley DE, Dehal PS, DeSantis TZ, Gihring TM, Lapidus A, Lin L-H, Lowry SR. 2008. Environmental genomics reveals a single-species ecosystem deep within Earth. Science 322(5899):275–278.

Cowen JP, Giovannoni SJ, Kenig F, Johnson HP, Butterfield D, Rappé MS, Hutnak M, Lam P. 2003. Fluids from aging ocean crust that support microbial life. Science 299(5603):120–123.

Craig H. 1961. Isotopic variations in meteoric waters. Science 133(3465):1702–1703.

D'Hondt S, Spivack AJ, Pockalny R, Ferdelman TG, Fischer JP, Kallmeyer J, Abrams LJ, Smith DC, Graham D, Hasiuk F, et al. 2009. Subseafloor sedimentary life in the South Pacific Gyre. Proc Natl Acad Sci USA 106(28):11651–11656.

Decoster MA, Maddi S, Dutta V, McNamara J. 2010. Microscopy and image analysis of individual and group cell shape changes during apoptosis. Microsc Sci Technol Appl Educ 2:836–843.

Doig F, Sherwood Lollar B, Ferris FG. 1995. Evidence for abundant microbial communities in Canadian Shield groundwaters – an in situ biofilm experiment. Geomicrob J 13(2):91–101.

Edwards KJ, Becker K, Colwell F. 2012. The deep, dark energy biosphere: intraterrestrial life on Earth. Annu Rev Earth Planet Sci 40(1):551–568.

Frape SK, Fritz P, McNutt RH. 1984. Water-rock interaction and chemistry of groundwaters from the Canadian Shield. Geochim Cosmochim Acta 48(8):1617–1627.

Goodwin AM. 1996. Principles of Precambrian Geology. London: Academic Press. 327 pp.

Heard AW, Warr O, Borgonie G, Linage B, Kuloyo O, Fellowes JW, Magnabosco C, Lau MCY, Erasmus M, Cason E, et al. 2018. Origin and ages of fracture fluids in the South African crust. Chemical Geol 283(3–4):287–296. doi.org/10.1016/l.chemgeo.2018.06.001.

Hoehler TM, Jorgensen BB. 2013. Microbial life under extreme energy limitation. Nat Rev Microbiol 11(2):83–94.

Holland G, Sherwood Lollar B, Li L, Lacrampe-Couloume G, Slater GF, Ballentine CJ. 2013. Deep fracture fluids isolated in the crust since the Precambrian era. Nature 497(7449):357–360.

Itävaara M, Nyyssönen M, Kapanen A, Nousiainen A, Ahonen L, Kukkonen I. 2011. Characterization of bacterial diversity to a depth of 1500 m in the Outokumpu deep borehole, Fennoscandian Shield. FEMS Microbiol Ecol 77(2):295–309.

Jannasch HW, Taylor CD. 1984. Deep-sea microbiology. Annu Rev Microbiol 38:487–514.

Kallmeyer J, Pockalny R, Adhikari RR, Smith DC, D'Hondt S. 2012. Global distribution of microbial abundance and biomass in subseafloor sediment. Proc Natl Acad Sci 109(40):15976–15977. 10.1073/pnas.1203849109.

Kelley DS, Karson JA, Früh-Green GL, Yoerger DR, Shank TM, Butterfield DA, Hayes JM, Schrenk MO, Olson EJ, Proskurowski G, et al. 2005. A serpentinite-hosted ecosystem: the Lost City Hydrothermal Field. Science 307(5714):1428–1434.

Kieft TL, Phelps TJ, Fredrickson JK. 2007. Drilling, coring, and sampling subsurface environments. In: Hurst, CJ, editor. Manual of Environmental Microbiology, Third Edition. Washington, DC: ASM Press, p 799–817.

Kieft TL, Walters CC, Higgins MB, Mennito AS, Clewett CFM, Heuer V, Pullin MJ, Hendrickson S, Van Heerden E, Sherwood Lollar B, et al. 2018. Dissolved organic matter compositions in 0.6-3.4 km deep fracture waters, Kaapval Craton, South Africa. Org Geochem 118:116–131.

Labonté JM, Field EK, Lau MCY, Chivian D, van Heerden E, Wommack KE, Kieft TL, Onstott TC. 2015. Single cell genomics indicates horizontal gene transfer and viral infections in a deep subsurface Firmicutes population. Front Microbiol 6:349.

Lau MCY, Kieft TL, Kuloyo O, Linage-Alvarez B, van Heerden E, Lindsay MR, Magnabosco C, Wang W, Wiggins JB, Guo L, et al. 2016. An oligotrophic deep-subsurface community dependent on syntrophy is dominated by sulfur-driven autotrophic denitrifiers. Proc Natl Acad Sci U S A 113(49):E7927–E7936.

Lehmann BE, Davis SN, Fabryka-Martin JT. 1993. Atmospheric and subsurface sources of stable and radioactive nuclides used for groundwater dating. Water Resour Res 29(7):2027–2740.

Li L, Wing BA, Bui TH, McDermott JM, Slater GF, Wei S, Lacrampe-Couloume G, Sherwood Lollar B. 2016. Sulfur mass-independent fractionation in subsurface fracture waters indicates a long-standing sulfur cycle in Precambrian rocks. Nat Commun 7:13252.

Lin L-H, Wang P-L, Rumble D, Lippmann-Pipke J, Boice E, Pratt LM, Sherwood Lollar B, Brodie EL, Hazen TC, Andersen GL, et al. 2006. Long-term sustainability of a high-energy, low-diversity crustal biome. Science 314(5798):479–482.

Lipp JS, Morono Y, Inagaki F, Hinrichs K-U. 2008. Significant contribution of Archaea to extant biomass in marine subsurface sediments. Nature 454(7207):991–994.

Lippmann J, Stute M, Torgersen T, Moser DP, Hall JA, Lin L, Borcsik M, Bellamy RES, Onstott TC. 2003. Dating ultra-deep mine waters with noble gases and ^{36}Cl, Witwatersrand Basin, South Africa. Geochim Cosmochim Acta 67(23):4597–4619.

Lippmann-Pipke J, Sherwood Lollar B, Niedermann S, Stroncik NA, Naumann R, van Heerden E, Onstott TC. 2011. Neon identifies two billion year old fluid component in the Witwatersrand Basin. Chem Geol 283(3–4):287–296.

Magnabosco C, Lin L-H, Dong H, Bomberg M, Ghiorse W, Stan-Lotter H, Pedersen K, Kieft TL, van Heerden E, Onstott TC. 2018a. The biomass and biodiversity of the continental subsurface. Nat Rev 11: 707–717.

Magnabosco C, Ryan K, Lau MCY, Kuloyo O, Sherwood Lollar B, Kieft TL, van Heerden E, Onstott TC. 2016. A metagenomic window into carbon metabolism at 3 km depth in Precambrian Continental Crust. Isme J 10(3):730–741.

Magnabosco C, Timmers PHA, Lau MCY, Borgonie G, Linage-Alvarez B, Kuloyo O, Alleva R, Kieft TL, Slater GF, van Heerden E, et al. 2018b. Fluctuations in populations of subsurface methane oxidizers in coordination with changes in electron acceptor availability. FEMS Microbiol Ecol 94(7). doi:10.1093/femsec/fiy089.

McDermott JM, Seewald JS, German CR, Sylva SP. 2015. Pathways for abiotic organic synthesis at submarine hydrothermal fields. Proc Nat Acad Sci 112:7668–7672.

McMahon S, Parnell J. 2014. Weighing the deep continental biosphere. FEMS Microbiol Ecol 87(1):113–120.

Michalski JR, Onstott TC, Mojzsis SJ, Mustard JF, Chan Q, Niles PB, Stewart Johnson S. 2017. The Martian subsurface as a potential window into the origin of life. Nat Geosci 3, 838–841.

Nakagawa S, Inagaki F, Suzuki S, Steinsbu B, Lever M, Takai K, Engelen B, Sako Y, Wheat C, Horikoshi K. 2006. Microbial community in black rust exposed to hot ridge flank crustal fluids. Appl Environ Microb 72(10):6789–6799.

NASEM (National Academies of Sciences, Engineering, and Medicine). 2018. An Astrobiology Science Strategy for the Search for Life in the Universe. London: The National Academies Press.

Oblinger JL, Koburger JA. 1975. Understanding and teaching the most probable number technique. J Milk Food Technol 38(9):540–545.
Onstott TC. 2016. Deep Life. Princeton: Princeton University Press. 486 pp.
Onstott TC, Lin L-H, Davidson M, Mislowack B, Borcsik M, Hall J, Slater G, Ward J, Sherwood Lollar B, Lippmann-Pipke J, et al. 2006. The origin and age of biogeochemical trends in deep fracture water of the Witwatersrand Basin. South Africa. Geomicrob J 23:369–414.
Orcutt BN, Bach W, Becker K, Fisher AT, Hentscher M, Toner BM, Wheat CG, Edwards KJ. 2011. Colonization of subsurface microbial observatories deployed in young ocean crust. ISME J 5(4):692–703.
Osburn MR, LaRowe DE, Momper LM, Amend JP. 2014. Chemolithotrophy in the continental deep subsurface: Sanford Underground Research Facility (SURF), USA. Front Microbiol 5: 610.
Pedersen K. 2000. Exploration of deep intraterrestrial microbial life: current perspectives. FEMS Microbiol Lett 185(1):9–16.
Pedersen K, Bengtsson AF, Edlund JS, Eriksson LC. 2014. Sulphate-controlled diversity of subterranean microbial communities over depth in deep groundwater with opposing gradients of sulphate and methane. Geomicrob J 31(7):617–631.
Proskurowski G, Lilley MD, Seewald JS, Früh-Green GL, Olson EJ, Lupton JE, Sylva SP, Kelley DS. 2008. Abiogenic hydrocarbon production at Lost City Hydrothermal Field. Science 319(5863): 604–607.
Purkamo L, Bomberg M, Nyyssönen M, Kukkonen I, Ahonen L, Itävaara M. 2015. Heterotrophic communities supplied by ancient organic carbon predominate in deep Fennoscandian bedrock fluids. Microb Ecol 69(2):319–332.
Purtschert R, Onstott TC, Jiang W, Lu Z-T, Muller P, Zappala J, Yokochi R, van Heerden E, Cason M, Lau M, et al. 2017. Underground production of ^{81}Kr detected in subsurface fluids. Goldschmidt Annual Meeting 2017, Paris, France, Aug. 13–18, 2017.
Santelli CM, Banerjee N, Bach W, Edwards KJ. 2010. Tapping the subsurface ocean crust biosphere: low biomass and drilling-related contamination calls for improved quality controls. Geomicrobiol J 27(2):158–169.
Schrenk MO, Brazelton WJ, Lang SQ. 2013. Serpentinization, carbon, and deep life. Rev Mineral Geochem 75(1):575.
Sheik CS, Reese BK, Twing KI, Sylvan JB, Grim SL, Schrenk MO, Sogin ML, Colwell FS. 2018. Identification and removal of contaminant sequences from ribosomal gene database: lessons from the Census of Deep Life. Front Microbiol 9:840.
Sherwood Lollar B. 2010. Far-Field Microbiology Considerations Relevant to a Deep Geologic Repository – State of Science Review. NWMO-TR-2010-23. Nuclear Waste Management Organization. 65 p.
Sherwood Lollar B, Lacrampe-Couloume G, Slater GF, Ward J, Moser DP, Gihring TM, Lin L-H, Onstott TC. 2006. Unravelling abiogenic and biogenic sources of methane in the Earth's deep subsurface. Chem Geol 226(3–4):328–339.
Sherwood Lollar B, Onstott TC, Lacrampe-Couloume G, Ballentine CJ. 2014. The contribution of the Precambrian continental lithosphere to global H_2 production. Nature 516(7531):379–382.
Sherwood Lollar B, Westgate T, Ward J, Slater GF, Lacrampe-Couloume G. 2002. Abiogenic formation of alkanes in the Earth's crust as a minor source for global hydrocarbon reservoirs. Nature 416(6880):522–524.
Simkus DN, Slater GF, Sherwood Lollar B, Wilkie K, Kieft TL, Magnabosco C, Lau MCY, Pullin MJ, Hendrickson SB, Wommack KE, et al. 2016. Variations in microbial carbon sources and cycling in the deep continental subsurface. Geochim Cosmochim Acta 173: 264–283.
Smith PE, Schandl ES, York D. 1993. Timing of metasomatic alteration of the Archean Kidd Creek massive sulfide deposit, Ontario, using ^{40}Ar–^{39}Ar laser dating of single crystals of fuchsite. Econ Geol 88(6):1636–1642.
Telling J, Voglesonger K, Sherwood Lollar B, Sutcliffe NC, Lacrampe-Couloume G, Edwards EA. 2018. Bioenergetic constraints on microbial hydrogen utilization in Precambrian deep crustal fracture fluids. Geomicrob J 35(2):108–119.
Thurston PC, Ayer JA, Goutier J, Hamilton MA. 2008. Depositional gaps in Abitibi greenstone belt stratigraphy: a key to exploration for syngenetic mineralization. Econ Geol 103(6):1097–1134.
Waite JH, Glein CR, Perryman RS, Teolis BD, Magee BA, Miller G, Grimes J, Perry ME, Miller KE, Bouquet A, et al. 2017. Cassini finds molecular hydrogen in the Enceladus plume: evidence for hydrothermal processes. Science 356(6334):155–159.
Ward J, Slater GF, Moser D, Lin L, Lacrampe-Couloume G, Bonin AS, Davidson M, Hall JA, Mislowack B, Bellamy RES, et al. 2004. Microbial hydrocarbon gases in the Witwatersrand Basin, South Africa: implications for the deep biosphere. Geochim Cosmo Acta 68(15):3239–3250.
Warr O, Sherwood Lollar B, Fellowes J, Sutcliffe NC, McDermott J, Holland G, Mabry JC, Ballentine CJ. 2018. Tracing ancient hydrogeological fracture network age and compartmentalisation using noble gases. Geochim Cosmochim Acta 222:340–362.
Young ED, Kohl IE, Sherwood Lollar B, Etiope G, Rumble D, Li S, Haghnegahdar MA, Schauble EA, McCain KA, Foustoukos DI, et al. 2017. The relative abundances of resolved $^{12}CH_2D_2$ and $^{13}CH_3D$ and mechanisms controlling isotopic bond ordering in abiotic and biotic methane gases. Geochim Cosmochim Acta 203:235–264.